Plasmonics (2013) 8:139–142
DOI 10.1007/s11468-012-9441-6

Detection of Change in Fluorescence Between Reactive Cyan and the Yellow Fluorophores Using a-SiC:H Multilayer Transducers

P. Louro · V. Silva · M. A Vieira · M. Vieira

Received: 10 May 2012 / Accepted: 26 August 2012 / Published online: 11 September 2012

Abstract The transducer consists of a semiconductor device based on two stacked -i-n heterostructures that were designed to detect the emissions of the fluorescence resonance energy transfer between fluorophores in the cyan (470 nm) and yellow (588 nm) range of the spectrum. This research represents a preliminary study on the use of such wavelength-sensitive devices as photodetectors for this kind of application. The device was characterized through optoelectronic measurements concerning spectral response measurements under different electrical and optical biasing conditions. To simulate the fluorescence resonance energy transfer (FRET) pairs, a chromatic time-dependent combination of cyan and yellow wavelengths was applied to the device. The generated photocurrent was measured under reverse and forward bias to read out the output photocurrent signal. A different wavelength-biasing light was also superimposed. Results show that under reverse bias, the photocurrent signal presents four separate levels, each one assigned to the different wavelength combinations of the FRET pairs. If a blue background is superimposed, the yellow channel is enhanced and the cyan suppressed, while under red irradiation, the opposite behavior occurs. So, under suitable biasing light, the transducer is able to detect separately the cyan and yellow fluorescence pairs. An electrical model, supported by a numerical simulation, supports the transduction mechanism of the device.

Keywords Optical sensors · Semiconductors · Photodiodes

P. Louro (✉) · V. Silva · M. A. Vieira · M. Vieira
Electronics Telecommunication and Computer Department, ISEL,
R. Conselheiro Emídio Navarro,
1949-014 Lisbon, Portugal
e-mail: plouro@deetc.isel.ipl.pt

P. Louro · V. Silva · M. A. Vieira · M. Vieira
CTS-UNINOVA,
Quinta da Torre, Monte da Caparica,
2829-516 Caparica, Portugal

M. Vieira
DEE-FCT-UNL,
Quinta da Torre, Monte da Caparica,
2829-516 Caparica, Portugal

Introduction

Fluorescence resonance energy transfer (FRET) is a process involving the radiationless transfer of energy from a "donor" fluorophore to an appropriately positioned "acceptor" fluorophore. The distance over which FRET can occur is limited to between 1 and 10 nm, and hence, this technique is used to demonstrate whether two types of molecules, labeled with a donor fluorophore and a receptor fluorophore, occur within 10 nm of each other. The determination of the distance between two molecular species is important in the field of medical and biological applications. This technique has grown in popularity due to the emergence of various fluorescent mutant proteins with shifted spectral properties [1, 2].

In this paper, we use wavelength-sensitive devices operating in the visible range to detect the cyan and yellow optical signals involved in FRET. The advantage of this type of transducer relies on the intrinsic optical filtering properties of the transducer associated with the photodetection ability. Thus, the use of this type of integrated devices discards the need of optical/mechanical filters to separate the wavelength of the emitted spectra and the use of an additional photodetector for each optical signal.

Experimental Details

The element sensor is a glass/TCO/a-SiC:H (p-i-n)/a-SiC:H (-p)/Si:H(-i)/SiC:H (-n)/TCO double heterostructure

produced by PECVD. Deposition conditions are described elsewhere [3]. The electrical contacts are made of a transparent contact oxide (TCO) to ensure light transmittance into the semiconductor sensitive device. The thickness (200 nm) and the absorption coefficient of the front photodiode (based on a-SiC:H) are optimized for short-wavelength collection and long-wavelength transmittance, and the thickness of the back one (1,000 nm) adjusted to achieve full absorption in the intermediate-wavelength region and high collection in the long-wavelength spectral section. As a result, both front and back diodes act as optical filters confining, respectively, the short- and the long-wavelength optical carriers, while the intermediate ones are absorbed across both [4]. In Fig. 1, the device configuration is depicted. Dual monochromatic light beams of 470 and 588 nm are directed to the device to simulate, respectively, the emitted cyan and yellow fluorescent signals of glucose oxidase from *Aspergillus niger* [1].

Results and Discussion

Glucose Oxidase Fluorescence Spectrum

In Fig. 2 is displayed the fluorescence emission spectrum of *A. niger* prepared with purified enzyme (specific activity of 125 U/mg protein) dissolved in 20 mM phosphate buffer, pH7.0 (5 mg/l). A wavelength of 450 nm was used as excitation source. The emission spectrum shows fluorescence in the range 480–600 nm with a peak located at 520 nm. Two peaks located at 518 and 562 nm originate from the deconvolution of the experimental data Gaussian fit, which corresponds respectively to the cyan and yellow emissions.

Device Spectral Sensitivity

Figure 3 displays the spectral photocurrent, measured along the visible spectrum, under reverse and forward bias without and with optical light bias of different wavelengths. Results show that without optical bias (dark lines), the use of reverse bias influences the photocurrent of the cyan wavelength emission, while for the yellow emission, it is independent of the electrical voltage applied to the device. On the other hand, under optical bias, either red (624 nm) or yellow

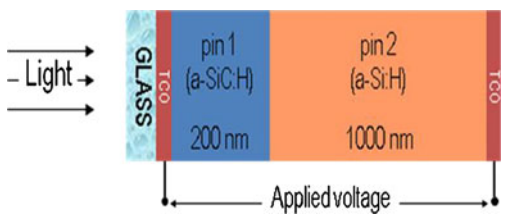

Fig. 1 Device configuration

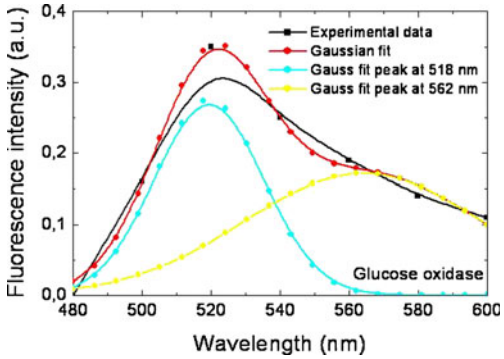

Fig. 2 Fluorescence emission of glucose oxidase

(588 nm), the photocurrent at −8 V exhibits the opposite behavior. Its magnitude remains constant at 470 nm, and at 588 nm, it decreases. Thus, the device sensitivity to the wavelengths of interest, i.e., 470 and 588 nm, can be tuned either by optical and electrical bias.

Device Output Photocurrent Signal

The photocurrent signal obtained at reverse and forward electric bias with and without red optical bias (624 nm) is displayed in Fig. 4 for both emission optical signals (470 nm and 588). As already seen in Fig. 3, the cyan emission signal (Fig. 4a) shows a strong dependence on the applied bias of the device. Under red optical bias, the signal is amplified with a magnitude factor of around 2. The yellow emission signal (Fig. 4b) shows a weaker dependence on the applied voltage and a strong attenuation under red optical bias.

A chromatic time-dependent wavelength combination (3,000 Hz) of both emission signals (470 and 588 nm) was used to simulate the FRET emission spectrum in the device. The output photocurrent, with (color lines) and without (dark lines) optical background light, is displayed in Fig. 5a and b under forward (dashed arrows) and reverse (solid arrows) voltages, respectively. The reference level was assumed to be the signal when all the input optical

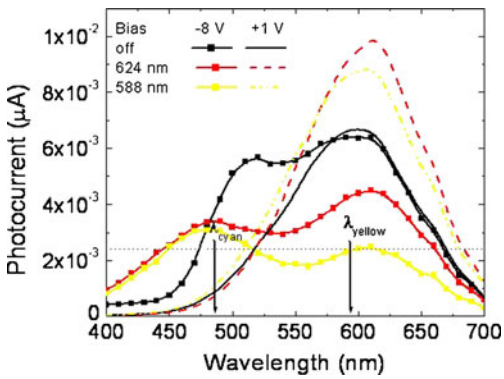

Fig. 3 Device spectral photocurrent under reverse and forward bias without and with red and yellow optical bias

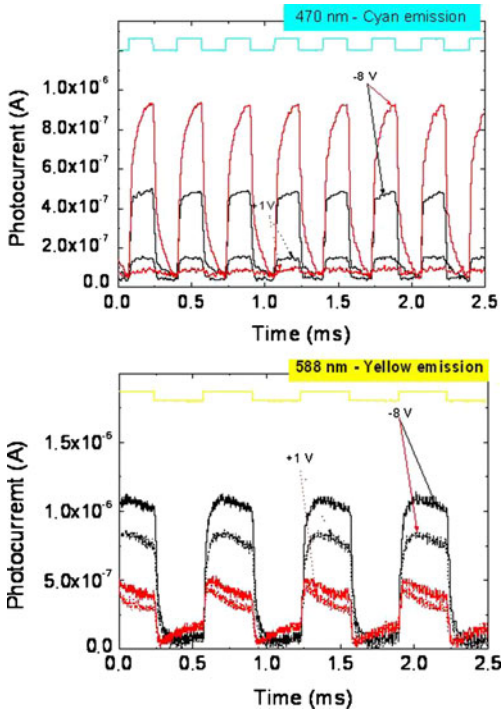

Fig. 4 Output photocurrent signal obtained at reverse (−8 V, *solid lines*) and forward (+1 V, *dashed lines*) bias without (*dark lines*) and with under red background light (*red lines*) with the **a** cyan (470 nm) and **b** yellow (588 nm) emission signals

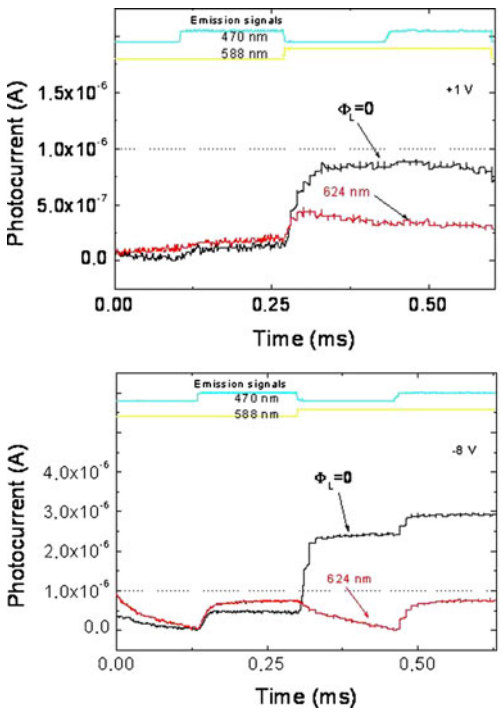

Fig. 5 Output photocurrent signals without (Φ_L=0) and with red optical bias (624 nm) at **a** forward bias (+1 V) and **b** reverse bias (−8 V). The optical signal waveforms are shown at the *top* of the figure

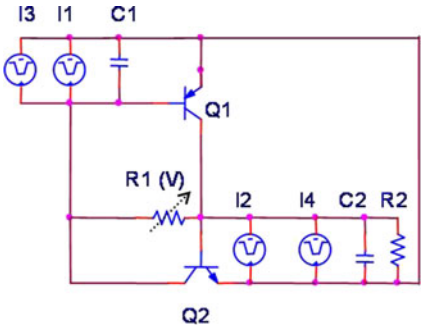

Fig. 6 Simplified ac equivalent electrical circuit of the device

signal channels are *off*. At the top of the figure, the individual optical signals are displayed to guide the eyes in relation to the different *on–off* states.

Under forward bias (Fig. 5a), the photocurrent signals with or without optical bias are similar, and their waveform follows the yellow fluorescence signal, due to the lower sensitivity of the device to the cyan light (Figs. 3 and 4). This feature allows immediate decoding of the yellow fluorescence signal. Under reverse bias (Fig. 5b), the photocurrent signal is more complex. Each waveform is four-level encoding (22) due to the different combinations of the input optical signals.

Once the yellow signal is decoded by the use of forward bias, the other fluorescence signal can be obtained from the photocurrent signal at −8 V taking into account the magnitude dependence on the applied bias (Fig. 4). To recover the cyan and yellow emission intensities, red optical bias was used. Under red irradiation, the yellow channel is quenched, and the cyan signal is amplified. So, the two highest levels in the photocurrent signal under 624 nm (Fig. 6b) correspond to the presence of the cyan light and the two lowest levels to its absence. The yellow channel is decoded under forward bias (Fig. 6a). By using this simple algorithm, the emission spectra can be recovered, in real time, and their ratios can be correlated with the distance between the fluorophores.

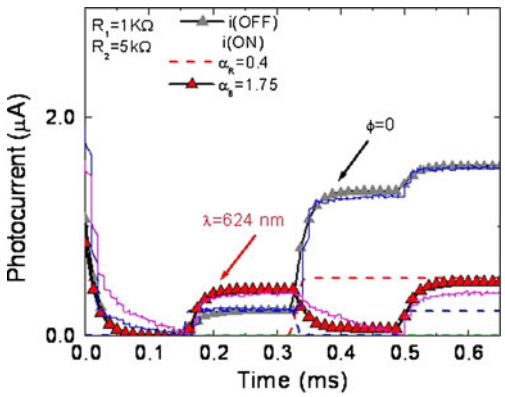

Fig. 7 Simulated photocurrent signal (*symbols*), input channels (*dashed lines*), and experimental signal (*solid lines*) under reverse bias (−8 V) and red optical bias (624 nm)

Electrical Model

Based on the experimental results and device configuration, an optoelectronic model was developed [5]. The device was modeled by a two single-tuned stage circuit with two variable capacitors and interconnected phototransistors through a resistor (Fig. 6). Two optical gate connections ascribed to the different light penetration depths across the front and back phototransistors were considered to allow independent yellow and cyan optical signal transmission.

Here, the charge stored in the space–charge layers is modeled by the capacitors C_1 and C_2. R_1 and R_2 model the dynamical resistances of the internal and back junctions under different *dc* bias conditions.

The operation is based upon the following principle: the flow of current through the resistor connecting the two front and back transistor bases is proportional to the difference in the voltages across both capacitors (charge storage buckets). So, it uses a changing capacitance to control the power delivered to the load acting as a state variable filter circuit.

In Fig. 7, the simulated current without and under red backgrounds is displayed (symbols) using the same test signal of Fig. 5. The input channels are also displayed (lines). To simulate the red background, current source intensities (input channels) were multiplied by the on/off ratio between the input channels with and without red optical bias. Good agreement between experimental and simulated data was observed.

The four expected levels, under reversed bias, and their reduction under red irradiation are clearly seen. Under the red background, the expected optical amplification of the cyan channel and the quenching of the yellow one were observed due to the effect of the active multiple-feedback filter when the back diode is light triggered.

Conclusions

We present a new semiconductor device based on an a-SiC:H p-i-n/p-i-n heterostructure for the detection of optical signals near the cyan and yellow regions of the visible spectrum, which can be used for the detection of the emission signals used in the FRET technique.

Two different modulated optical signals were used to simulate the emission signals of the fluorophores used in FRET. The output emission spectrum was analyzed by reading out the photocurrent generated by the device. The transducer mechanism was explained by an electrical model supported by a numerical simulation.

Future work comprises the use of lower-power intensities for the simulated emission signals in order to reach the same range of the ones produced during the FRET phenomenon. In a further stage, tests with emission fluorescence signals from different samples of glucose oxidase must also be done.

Acknowledgments This work was supported by PTDC/EEA-ELC/111854/2009 and PTDC/EEA-ELC/120539/2010.

References

1. LaVan DA, McGuire T, Langer R (2003) Nat Biotechnol 21 (10):1184–1191
2. D. Grace (2008) Medical product manufacturing news, 12, 2008, 22–23
3. Vieira M, Fantoni A, Fernandes M, Louro P, Lavareda G, Carvalho CN (2007) Thin Solid Films 515(19):7566–7570
4. Louro P, Vieira M, Vygranenko Y, Fantoni A, Fernandes M, Lavareda G, Carvalho Mat N (2007) Res Soc Symp Proc 989:A12.04
5. Vieira MA, Vieira M, Costa J, Louro P, Fernandes M, Fantoni A (2010) Sensors & Transducers Journal 9:96–120, Special Issue, December 2010